

First implementation of Quantum Process Tomography in MRI

Nicolas Boulant¹, Aurelien Massire¹, and Alexis Amadon¹
¹Neurospin, CEA, Saclay, Ile de France, France

Target audience: MRI physicists

Purpose: Tailored radiofrequency pulses exploiting parallel transmission have already been shown to greatly mitigate B₁ and B₀ inhomogeneities at ultra high field. In their investigations, radiofrequency pulse designers often use flip angle measurements to validate their new developments. However when the objective is to implement true target matrix rotations, as for instance in the spin-echo sequence, those measurements provide only partial information about the operation. The method of Quantum Process Tomography (QPT)¹ was invented in the field of Quantum Information Processing to characterize unknown, very often non unitary, dynamics. For the first time in MRI, we report its implementation at 7 Tesla in order to verify the correct implementation of a 180° refocusing pulse designed using parallel transmission (pTX).

Methods: The idea is to apply the operation to be characterized to different input magnetization states forming a set of linearly independent vectors, measure the corresponding output states, and retrieve the linear mapping via a mathematical recipe². The operation we characterized was a 3D 180° refocusing pulse designed using the GRAPE method³ and parallel transmission on a 16 cm diameter water phantom (0.25 mM Dotarem, 6 g/L NaCl). Experiments were carried out at 7 Tesla using a Magnetom scanner (Siemens, Erlangen, Germany) and a home-made 8 channels pTX array coil. Although in general the procedure can characterize non-unitary dynamics, here for simplicity and due to the fact that the RF pulse was short compared to T₁ and T₂, we assumed the dynamics to be unitary, which as a consequence made the number of necessary measurements lower. First an AFI⁴ sequence was implemented to characterize a given reference excitation pattern. Second, a GRE sequence with the same excitation pattern was implemented with TR >> T₁. In that case the magnitude of the signal was simply $\rho\alpha(r)\exp(-TE/T_2^*)\sin(FA)$ where ρ , α and FA are the spin density, reception sensitivity and flip angle respectively. Knowing the flip angle in every voxel thanks to the AFI sequence then allows to compute $\rho\alpha(r)\exp(-TE/T_2^*)$ and to normalize all subsequent data with it. Last, this allows to compute the magnetization state at the end of the excitation pulse for each voxel: $[M_x^{in} M_y^{in} M_z^{in}] = [\sin(FA)\cos(\phi) \sin(FA)\sin(\phi) \cos(FA)]$, where ϕ is the measured phase unwound with the measured ΔB_0 evolution during TE. This constitutes the first input state for the subsequent refocusing pulse. Two other independent states were simply generated by shifting the phase of each RF transmitter, or equivalently ϕ , by 45° and 90°, thereby yielding the second and third input states. Finally, these pulses were concatenated in front of our tailored 180° refocusing pulse and inserted into their respective GRE sequence. Likewise, the measured signal allowed to determine $[M_x^{out} M_y^{out} M_z^{out}]$ in each case by using the output signal, phase and normalization condition, again assuming unitary dynamics. The procedure thus can be expressed with the following matrix equation:

$$\begin{bmatrix} M_x^{Out,0} & M_x^{Out,45} & M_x^{Out,90} \\ M_y^{Out,0} & M_y^{Out,45} & M_y^{Out,90} \\ M_z^{Out,0} & M_z^{Out,45} & M_z^{Out,90} \end{bmatrix} = \begin{bmatrix} \text{Rotation} \\ \text{matrix} \end{bmatrix} \begin{bmatrix} M_x^{In,0} & M_x^{In,45} & M_x^{In,90} \\ M_y^{In,0} & M_y^{In,45} & M_y^{In,90} \\ M_z^{In,0} & M_z^{In,45} & M_z^{In,90} \end{bmatrix},$$

where the numbers in superscript refer to the used phase configuration. Our first estimation of the rotation matrix then simply is $Res = [Out][In]^{-1}$. Nevertheless, because of experimental errors and not perfectly unitary dynamics, we used the polar decomposition to obtain the closest rotation matrix consistent with the data. This procedure returns: $Rot = Res(\sqrt{Res'Res})^{-1}$, where Res' here is the Hermitian conjugate of Res .

Results: In Figure 1 we provide the results of QPT and compare them with our numerical Bloch simulations. Our designed 180° refocusing pulse was 4.65 ms long (Figure 1.f), i.e. short compared to T₁ and T₂ (~600 ms). Rotation angles and (α,β) Cayley Klein parameters could be extracted from the rotation matrix in every voxel by inspecting its eigenvalues and eigenvectors. Figures 1.a.b confirm that the rotation angles were close to 180° while Figures 1.c.d confirm both a rotation angle close to 180° and a pure transverse rotation axis ($1-|\beta|^2 = 0$), thereby validating both the pulse design and our implementation of QPT.

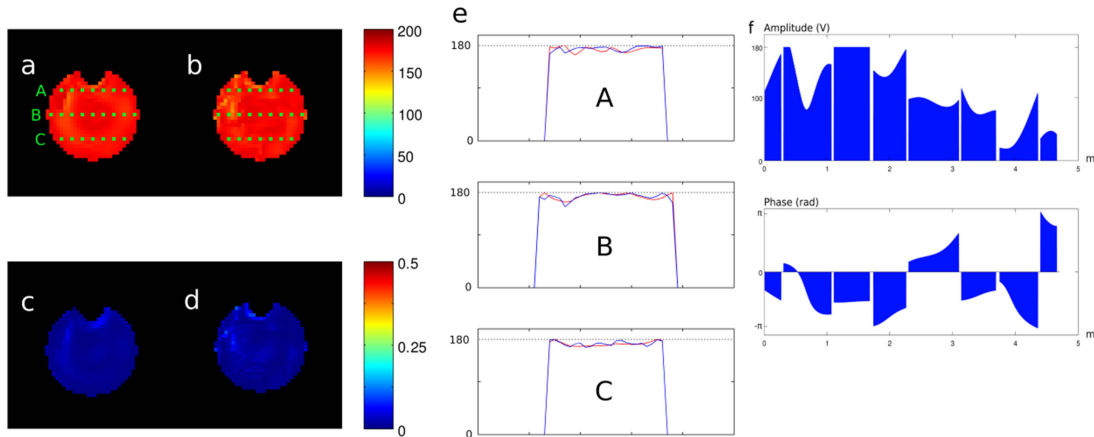


Figure 1. Quantum process tomography results (axial slices) with a: Measured rotation angle (in °). b: Simulated rotation angle (in °). c: Measured $1-|\beta|^2$. d: Simulated $1-|\beta|^2$. e: 1-D profiles along several cuts through the in-plane rotation angle profile (red: measured, blue: simulated). f: Channel #1 waveform of the refocusing pulse (amplitude and phase).

Conclusion: We have implemented for the first time QPT in MRI. This method characterizes the whole implemented operation (= process) as opposed to the state (= magnetization vector). To simplify the analysis, and because the experiment was performed on a water phantom, long GRE acquisitions were used. The procedure however seems doable in-vivo with shorter acquisition times as long as the signal is proportional to $\sin(FA)$, for instance when $FA \ll \theta_E$ (Ernst angle) even if $TR \ll T_1$.

References: 1. Nielsen MA, Chuang IL. Quantum Computation and Quantum Information. Cambridge University Press, 2000. 2. Havel TF. J. Math. Phys. 44 (2003) 534. 3. Khaneja N, Reiss T, Kehlet C, Schulte-Herbrüggen T, Glaser SJ. J. Magn. Reson. 172 (2005) 296-305. 4. Yarnykh V, Magn. Reson. Med. 57 (2007) 192-200.

Acknowledgments: The research leading to these results has received funding from the European Research Council under the European Union's Seventh Framework Program (FP7/2013-2018) / ERC Grant Agreement n. 309674.